CHEMISTRY
A EUROPEAN JOURNAL

DOI: 10.1002/chem.200700444

Nanoscale Metal Coordination Macrocycles Fabricated by Using "Dimeric" Dipyrrins

Hiromitsu Maeda*[a, b] and Takashi Hashimoto[a]

Abstract: Covalently linked dipyrrin (dipyrromethene) dimers have afforded nanoscale [2+2]-type neutral coordination macrocycles with a diagonal of about 1.6 nm. Two moieties of the achiral dipyrrin–Zn^{II} complex yield the chiral coordination macrocycles as minor species, as well as major *meso* stereoisomers by the covalent linkages. Tetrahedral Zn^{II} coordination by using acyclic ligands enables the dipyrrin–metal complex units to readily rotate and pass through the cavity of the nanorings in order to reveal the transitions between the chiral and achiral isomers.

Keywords: chirality · macrocycles · metallacycles · N ligands · nanostructures

Introduction

Coordination cavities fabricated using the metal complexation of organic molecules are fascinating and widely investigated as host species to recognize guest molecules for catalyzing particular reactions.[1] Metal-organic microporous materials (MOMs) based on coordination polymers using ligands such as oligopyridyl derivatives have been found to encapsulate gas molecules.[2,3] On the other hand, discrete coordination macrocycles and cages with/without positive charge(s) have been investigated as isolated spaces to bind specific molecules and ions in solution.[4–6] With regard to ligand moieties, dipyrrins (dipyrromethenes) are comprised of two pyrroles bridged by an sp^2-*meso* carbon, similar to a half-porphyrin unit, and essential π-conjugated bidentate monoanionic ligands for metal ions.[7–11] As compared to using porphyrins as rigid macrocycles, the use of dipyrrins as acyclic ligands can afford flexible metal coordination environments. Recently, we reported the formation of coordination polymers and nanoscale spherical architectures using $Zn(OAc)_2$ and "dimeric" dipyrrin derivatives in which two dipyrrin units were bridged by phenylethynyl linkers.[12] According to the metal complexation conditions and the angles of the linkages, coordination oligomers would form infinite linear or discrete structures. In this article, we report the [2+2]-type coordination macrocycles by using the all-*meta*-bridged derivatives of dimeric dipyrrins under modified conditions.

[a] Prof. Dr. H. Maeda, T. Hashimoto
Department of Bioscience and Biotechnology
Faculty of Science and Engineering, Ritsumeikan University
Kusatsu 525-8577 (Japan)
Fax: (+81) 77-561-2659
E-mail: maedahir@se.ritsumei.ac.jp

[b] Prof. Dr. H. Maeda
Department of Materials Molecular Science
Institute for Molecular Science (IMS)
Okazaki 444-8787 (Japan)

Supporting information for this article is available on the WWW under http://www.chemeurj.org/ or from the author.

Results and Discussion

Synthesis and characterization of dipyrrin dimers and metal complexes: As previously reported,[10,12] dimeric dipyrrin **1a** was synthesized by performing the Sonogashira coupling reaction of 1,3-diethynylbenzene and 3-bromobenzaldehyde, followed by condensation with pyrrole and subsequent DDQ oxidation (Scheme 1a). Similar procedures were performed in the reaction using α-alkylpyrroles to afford dipyrrin dimers **1b** and **1c** in yields of 21 and 19%, respectively, from a diformyl intermediate. The chemical identities of **1a–c** were confirmed by ^{1}H NMR spectroscopy and FAB-MS spectrometry; UV/Vis absorption spectra of these derivatives in $CHCl_3$ were observed at $\lambda = 435$, 446, and 450 nm, respectively, suggesting almost no electronic interactions between the two dipyrrin moieties bridged by a spacer.

Next, we investigated the coordination chemistry of dimeric dipyrrins. When $Zn(OAc)_2$ was added to the $CHCl_3$ solution of **1a** with 0.5 equiv of pyrene (with a length of ca. 9 Å) as a template molecule and the mixture was heated to the reflux temperature for two days, the solution color slightly darkened. Purification by silica gel column chroma-

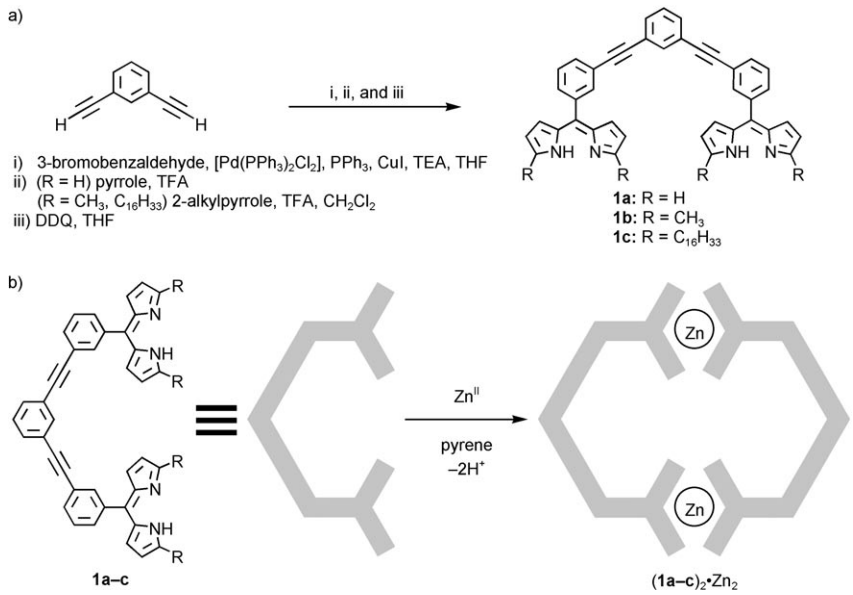

Scheme 1. a) Synthesis and b) Zn^{II} complexation of dipyrrin "dimers" **1a–c**.

tography and recrystallization from $CHCl_3$/hexane afforded a yellow solid in a yield of 77% (Scheme 1b). ESI-TOF-MS analyses of the complexes with $AgClO_4$ (5 equiv) as a cation source revealed the exact composition of the Zn^{II} complexes of discrete [2+2]-type coordination macrocycles at, for example, *m*/*z* 1249.26 and 1355.16 for $\mathbf{1a}_2{\cdot}Zn_2{\cdot}H^+$ (exact mass: 1249.26) and $\mathbf{1a}_2{\cdot}Zn_2{\cdot}Ag^+$ (1355.16), respectively. Similar results were further supported by a GPC-HPLC analysis with a single peak. Other solvents such as THF and toluene with pyrene and other template molecules like C_{60} are also suitable to synthesize these [2+2] complexes. Under these conditions, discrete higher homologues have not been obtained. In contrast, it is known that the Zn^{II} complexation of **1a** without a template molecule in THF/H_2O at room temperature yields 1D coordination polymers and submicrometer-scale spherical particles with dents.[12] The UV/Vis absorption spectrum of $\mathbf{1a}_2{\cdot}Zn_2$ in $CHCl_3$ shows the absorption maximum (λ_{max}) at 486 nm, with a "shoulder" at about 465 nm, derived from the mixture of stereoisomers described below. Further, the fluorescence emission of $\mathbf{1a}_2{\cdot}Zn_2$ at 505 nm (λ_{ex} = 486 nm) in the same solvent reveals a comparable Stokes shift than those in the other Zn^{II} complexes (e.g., λ_{max} = 486 nm and λ_{em} = 501 nm of the *meso*-mesityl–dipyrrin–Zn^{II} complex in $CHCl_3$). Similar trends were observed in other derivatives **1b**,**c**.

Stereoisomers formed using tetrahedral Zn^{II} and acyclic ligands: Binuclear Zn^{II} complexes are expected to afford two chiral centers due to the tetrahedral geometry of a Zn^{II} ion.[8c,13] In the [2+2]-type complexes such as $\mathbf{1a}_2{\cdot}Zn_2$, two metal-recognition sites (dipyrrin groups) are "strapped" by phenylethynyl linkers; therefore, the Zn^{II} complexes are classified into three types of stereoisomers (two diastereomers): achiral (*meso*, ΛΔ) and chiral (ΛΛ and ΔΔ),[14] as seen in the optimized structures of $\mathbf{1a}_2{\cdot}Zn_2$ (Figure 1) and $\mathbf{1b}_2{\cdot}Zn_2$ at the AM1 level.[15]

The ^{1}H NMR spectrum in addition to the MS analysis revealed 1) the formation of [2+2]-coordination macrocycles and 2) the existence of diastereomers derived from cyclization. The two sets of signals

Figure 1. Possible three stereoisomers, a) achiral (*meso*), b) chiral (ΛΛ), and c) chiral (ΔΔ), of $\mathbf{1a}_2{\cdot}Zn_2$, optimized at the AM1 level.

with different integrations at a ratio of 4.6:1 derived from the integrals of β-CH were observed in the ^{1}H NMR spectrum of $\mathbf{1a}_2{\cdot}Zn_2$ in $CDCl_3$ (Figure 2). A similar trend was observed in $\mathbf{1b}_2{\cdot}Zn_2$ with a ratio of 3.2:1. The formation of coordination nanorings is further suggested by the split chemical shifts ($\Delta\delta$) in each dipyrrin β-CH signal of $\mathbf{1a}_2{\cdot}Zn_2$ between the relative "internal" (H^k, H^l, and H^m) and "external" (H^h, H^i, and H^j) protons (e.g. $\Delta\delta = 0.028$ ppm at the signals around 6.71 ppm (H^h and H^k) as the "major" set) derived from the cavity. All the proton signals of the major isomer as the *meso* one (see below) are assigned using ^{1}H–^{1}H COSY and ROESY, which show correlations between H^f–H^h and H^g–H^k (see Supporting Information). The 2D NMR spectra also revealed the resonances of dipyrrin α-CH at δ 7.58 (H^j) and 7.50 (H^m) ppm, which afford $\Delta\delta = \approx 0.08$ ppm; these values are greater than those of β-CH (0.028 and 0.013 ppm). In the case of α-CH (H^i and H^m) and β-CH (H^i and H^l), the external protons (H^i and H^j) are observed in the downfield region as compared to the internal ones (H^l and H^m). Further, the sets of major signals derived from pyrrole β-CH (H^h and H^k) at around 6.71 ppm in $\mathbf{1a}_2{\cdot}Zn_2$ are observed in the upfield region than that in the corresponding "minor" ones (ca. 6.77 ppm). The $\Delta\delta$ value between the internal and external β-CH signals of the minor

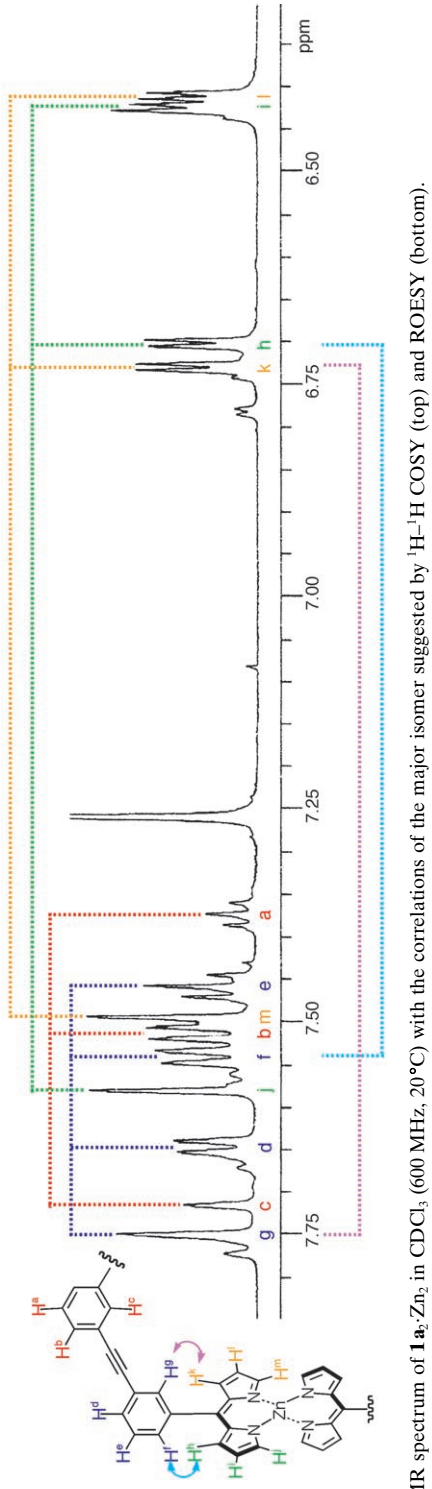

Figure 2. ^{1}H NMR spectrum of $\mathbf{1a}_2$·Zn_2 in $CDCl_3$ (600 MHz, 20 °C) with the correlations of the major isomer suggested by ^{1}H–^{1}H COSY (top) and ROESY (bottom).

species, which partially overlap with the major signals, is estimated to be 0.043 ppm; this value is slightly greater than that of the major isomer.

The chiral HPLC analysis of $\mathbf{1a}_2$·Zn_2 (Sumichiral OA-3100, $CHCl_3$/hexane 1:2 containing ca. 0.2 % EtOH as the eluent) revealed that the major and minor fractions are achiral (*meso*) and chiral stereoisomers, respectively.[16] These results are also consistent with the existence of two types of diastereomers, as shown in Figure 1. Interestingly, the UV/Vis absorption spectrum of each isomer differs as seen in the absorption maxima at 484 and 467 nm for the major and minor fractions (crude in both the cases), respectively. The other complexes, $\mathbf{1b}_2$·Zn_2 and $\mathbf{1c}_2$·Zn_2, revealed a more distinct resolution with a total of three peaks among the three stereoisomers in which chiral enantiomers are considered to be the minor species. Although tetrahedral dipyrrin–Zn^{II} moieties are achiral, the covalent linkages of the *same* helicities afford "chiral rings", which would be the potential receptors for the chiral species.[14a] Such chirality observed in the minor isomers is a unique property derived from the distorted geometries of dipyrrin complexes as opposed to those of planar porphyrins.

However, the Cotton effect observed in the CD spectrum has not been observed in one of the enantiomers in $\mathbf{1b}_2$·Zn_2, possibly due to the interconversion between the stereoisomers. Actually, equilibrium between the diastereomers is observed in $\mathbf{1a}_2$·Zn_2 and $\mathbf{1b}_2$·Zn_2 by the ^{1}H NMR spectral changes ($CDCl_3$) for various temperatures; in these complexes, the ratios of *meso* and chiral isomers are 4.1:1 and 2.7:1, respectively, at −60 °C. At higher temperatures, the ratio of *meso* isomers is further increased and the chemical shifts ($\Delta\delta$) between the internal and external β-CH signals at around 6.6–6.7 ppm are smaller in each isomer: for example, $\Delta\delta = 0.015$ and 0.055 ppm in the *meso* isomer of $\mathbf{1a}_2$·Zn_2 at 60 and −60 °C, respectively. The equilibrium constants K between the chiral and *meso* isomers of $\mathbf{1a}_2$·Zn_2 are 4.6, 4.4, and 4.1 at 20, −20, and −60 °C, respectively, to afford ΔG^0 of −3.7, −3.1, and −2.5 kJ mol^{-1}. On the other hand, the K (and ΔG^0) values of $\mathbf{1b}_2$·Zn_2 are 3.2 (−2.8), 3.0 (−2.3), and 2.7 (−1.7 kJ mol^{-1}) at each temperature. From these data and the van 't Hoff plots, the thermodynamic parameters (ΔH^0 and ΔS^0) could be estimated as 0.75 kJ mol^{-1} and 15 J K^{-1} mol^{-1} for $\mathbf{1a}_2$·Zn_2 and 1.1 kJ mol^{-1} and 13 J K^{-1} mol^{-1} for $\mathbf{1b}_2$·Zn_2; this suggests that for both the cases, the chiral isomers are slightly thermodynamically more stable than the achiral ones, particularly for methyl-substituted $\mathbf{1b}_2$·Zn_2.[17]

The rate constants (k) of the rotation of the dipyrrin moieties of $\mathbf{1a}_2$·Zn_2 and $\mathbf{1b}_2$·Zn_2 from each achiral to chiral isomer have been determined to be 0.5 and 0.3 s^{-1}, respectively, by means of the spin saturation transfer method ($CDCl_3$, 20 °C), irradiating one of the β-CH signals of the minor isomers.[18] The slightly larger k value in $\mathbf{1a}_2$·Zn_2 might be attributed to the less sterical hindrance than in methyl-substituted $\mathbf{1b}_2$·Zn_2. Such slow transitions between the stereoisomers are consistent with the results of the HPLC analysis to yield the mixture again after a temporary

resolution. The transitions between the *meso* and chiral isomers would be achieved by the 90° rotation of one of the two dipyrrin–metal units, wherein one of the four β-CH passes through a nanoscale ring cavity, such as that in molecular motors or vehicles.[19]

Solid-state structure and assembly of coordination nanorings: The solid-state structure of *meso*-type diastereomer $\mathbf{1a}_2{\cdot}Zn_2$ as a major stereoisomer has been revealed by X-ray diffraction analysis using a single crystal from the mixture of two diastereomers (Figure 3a). The coordination macrocycle, showing the distorted hexagonal cavity, consists of dimeric dipyrrins and Zn^{II} cations. The dihedral angle between the two dipyrrin moieties (a–b) is 89.18°, that is, they are almost perpendicular to each other. The distance between two Zn^{II} cations is 12.35 Å, and the averaged distances between the parallel dipyrrin moieties (a–a′ and b–b′) are 6.36 and 10.93 Å, respectively; they exhibit an almost rectangular geometry (Figure 3b), which is distorted as compared to the optimized structure (Figure 1a). The distances between the dipyrrins' "inner" carbons (C1–C2′) and spacers' inner carbons (C3–C3′) are estimated to be 7.63 and 16.23 Å, respectively, and the dihedral angles between the bridged-phenyl moieties (c–d and d–e) are 30.50 and 47.34°, respectively. Here, like Rebek's molecular capsules,[20] the two THF molecules used as the solvent are encapsulated in a nanoscale cavity assisted by the interaction of oxygen with phenyl (d) CH for a distance of 3.49 Å, although the O site shows no coordination with Zn^{II}, as also seen in the phenylethynyl-substituted dipyrrin–Zn^{II} complex.[12] Like the [3+3]-type complexes[8] and the assemblies in the solid state,[9] the coordination nanorings in this report are the first examples of the [2+2]-dipyrrin assemblies with a promising guest-binding cavity, which are different from the [2+2]-type helical supramolecular assemblies based on dipyrrin derivatives.[8]

Further, intermolecular donor/donor- and acceptor/acceptor-type CH-π interactions are observed in C4′-H of dipyrrin and C5′-H of the aryl ring to dipyrrin plane (a) with distances of 3.29 and 3.38 Å, respectively (Figure 3c). Therefore, a phenyl moiety (c,c′) of the neighboring "nanoring" seems to be encapsulated in a cavity. Four hydrogen-bonding donating sites and four accepting π planes in each coordination macrocycle (e.g., ring-A (gray)) form the 2D supramolecular networks with four macrocycles in the neighboring layers (ring-B (orange) as hydrogen-bonding donors and ring-C (blue) as acceptors) using a total of eight interactions (Figure 3e,f). In the same layer, a macrocycle (A) interacts with the four neighboring macrocycles (ring-D (purple) and ring-E (green)) using the donor/acceptor-type CH–π interactions between the ethynyl units and aryl C6–H (3.39 Å) and dipyrrin C8–H (3.67 Å) (Figure 3d–f). The macrocycles are stacked with those in the other layers and "connected" with those in the same layer to yield the molecular "bricks" in the solid states.

Conclusion

The [2+2]-coordination macrocycles based on the "dimeric" dipyrrin derivatives have been formed using a template molecule. Two moieties of achiral Zn^{II}–dipyrrin complex yield the chiral coordination macrocycles as the minor species, as well as major *meso* stereoisomers, by the covalent linkages. Tetrahedral Zn^{II} coordination using acyclic ligands enables the dipyrrin–metal complex units to readily rotate and pass through the cavity of nanoring to reveal the transitions between the chiral and achiral isomers. Presumably, this observation—derived from the combination of dipyrrin derivatives and Zn^{II} cations—is not characteristic to planar coordination moieties. The preliminary studies of dipyrrins with other metal ions such as Cu^{II} and Ni^{II} highlight similar trends such as those in Zn^{II} complexes, and the chemistry similar to other transition-metal complexes including $\mathbf{1a}_2{\cdot}Cu_2$ and $\mathbf{1a}_2{\cdot}Ni_2$ is currently being investigated by our group. In sharp contrast to Zn^{II} complexes, any diastereomers in $\mathbf{1a}_2{\cdot}Ni_2$ were not observed in the ^1H NMR ($CDCl_3$) spectra, possibly due to the square-planar geometry of Ni^{II}. Further, as expected from the binding of the solvent molecules in the solid state, the synthesis and investigation of derivatives to encapsulate guest species in solution are also now in progress.

Experimental Section

General procedures: Starting materials were purchased from Wako Chemical Co., Nacalai Chemical Co., and Aldrich Chemical Co. and used without further purification unless otherwise stated. UV-visible spectra were recorded on a Hitachi U-3500 spectrometer. NMR spectra used in the characterization of products were recorded on a JEOL ECA-600HR 600 MHz spectrometer. All NMR spectra were referenced to solvent. Fast atom bombardment mass spectrometric studies (FAB-MS) were made using a JOEL GCmate instrument in the positive ion mode with a 3-nitrobenzylalcohol matrix. Electrospray ionization time-of-flight mass spectrometric studies (ESI-TOF-MS) were made using a Bruker microTOF focus instrument in the positive ion mode with a silver(I) perchlorate. Matrix assisted laser desorption/ionization time-of-flight mass spectrometric studies (MALDI-TOF-MS) were made using a SHIMADZU MALDI-II instrument in the positive ion mode with a 7,7,8,8-tetracyanoquinodimethane matrix. TLC analyses were carried out on aluminum sheets coated with silica gel 60 (Merck 5554). Column chromatography was performed on Sumitomo alumina KCG-1525 and Wakogel C-300. GPC-HPLC and Chiral-HPLC analyses were performed with a JASCO PU-980 instrument (JAIGEL 4H-AF, 3H-AF, and 2.5H-AF) and a SHIMADZU LC-6AD instrument (SUMICHIRAL OA-3100), respectively. Synthesis of compound **1a** has been reported in the literature procedures.[12]

Synthesis and spectroscopic data for dipyrrin dimers, their precursors, and metal complexes

1,3-Bis(di-5-methylpyrrol-2-ylmethylphenylethynyl)benzene (DPM-1b): 1,4-Bis(4-formylphenylethynyl)benzene (42.8 mg, 0.13 mmol) and 2-methylpyrrole (102.6 mg, 1.26 mmol) were dissolved in CH_2Cl_2 (11 mL) and degassed by bubbling with nitrogen for 20 min. Trifluoroacetic acid (3.0 μL, 0.018 mmol) was added and the solution was stirred for 20 min. The reaction mixture was diluted with CH_2Cl_2 (20 mL), washed with 0.1 M NaOH aq. (20 mL) and brine (20 mL), then dried over Na_2SO_4, and evaporated to remove CH_2Cl_2. The remaining pyrrole was removed by vacuum distillation with gentle heating. The product was purified by

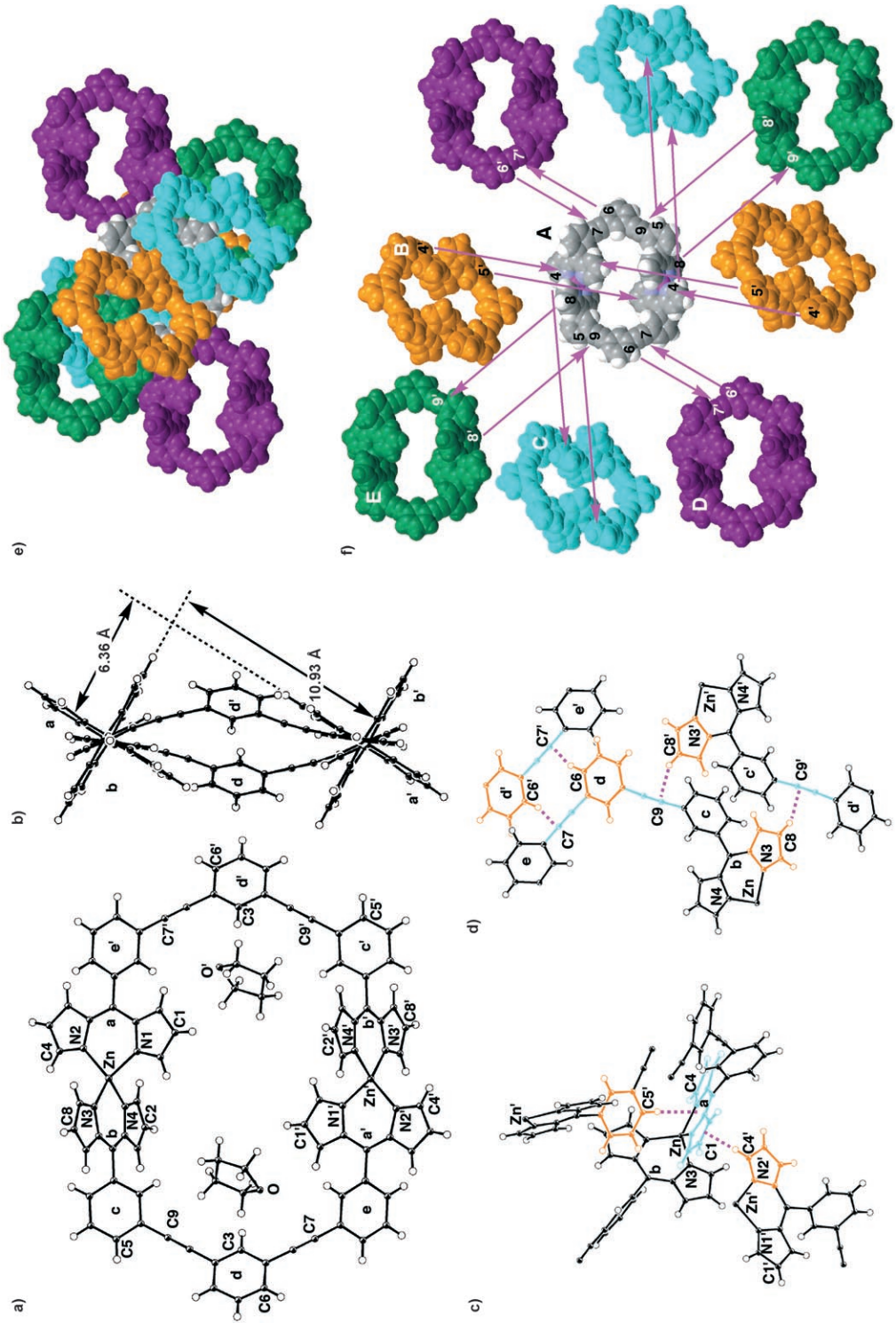

Figure 3. a,b) ORTEP drawing (top and side views, 50 % probability of forming ellipsoids), c,d) CH–π interactions in the neighboring macrocycles, e) packing diagram, and f) arrangement of nine molecules with the CH–π interactions (represented by the arrows from hydrogen-bonding donors to acceptors) of the X-ray single crystal structure of $\mathbf{1a}_2{\cdot}Zn_2$. Solvent molecules (THF) are omitted in b–f) for clarity. The atoms and planes of the other half unit in a,b) and the "neighboring" moieties in c)–f) are labeled using prime symbols. Selective bond lengths [Å] and angles [°]: 1.958(6) (Zn–N1), 1.966(5) (Zn–N2), 1.947(6) (Zn–N3), 1.974(6) (Zn–N4), 94.1(2) (N1-Zn-N2), 119.9(2) (N2-Zn-N3), 94.7(3) (N3-Zn-N4), 112.4(2) (N4-Zn-N1), 117.7(3) (N1-Zn-N3), 119.6(2) (N2-Zn-N4).

silica gel column chromatography (50% hexane/CH_2Cl_2) and recrystallized from CH_2Cl_2/hexane to afford **DPM-1b** (68.1 mg, 85%) as a dark red solid. R_f=0.67 (50% hexane/CH_2Cl_2); ^{1}H NMR (600 MHz, $CDCl_3$, 20°C): δ=7.68 (brs, 4H; NH), 7.45 (dd, J=7.8, 1.8 Hz, 2H; ArH), 7.43 (s, 1H; ArH), 7.42 (ddd, J=7.2, 1.2, 1.2 Hz; 2H, ArH), 7.33–7.29 (m, 3H; ArH), 7.23–7.21 (m, 2H; ArH), 5.81 (dd, J=3.0, 3.0 Hz, 4H; pyrrole-H), 5.77 (dd, J=3.0, 3.0 Hz, 4H; pyrrole-H), 5.36 (s, 2H; *meso*H), 2.22 ppm (s, 12H; CH_3); FABMS: m/z (%): calcd for $C_{44}H_{38}N_4$: 622.31; found: 622.4 $[M]^+$ (100), 623.4 $[M+1]^+$ (47).

1,3-Bis(bis-5-hexadecylpyrrol-2-ylmethylphenylethynyl)benzene (DPM-1c): 1,4-Bis(4-formylphenylethynyl)benzene (19.5 mg, 0.06 mmol) and 2-hexadecylpyrrole (160.2 mg, 0.55 mmol) was dissolved in CH_2Cl_2 (7.0 mL) and degassed by bubbling with nitrogen for 20 min. Trifluoroacetic acid (2.0 μL, 0.012 mmol) was added and the solution was stirred for 40 h. The reaction mixture was diluted with CH_2Cl_2 (50 mL), washed with 0.1 M NaOH aq. (50 mL) and brine (50 mL), then dried over Na_2SO_4, and evaporated to remove CH_2Cl_2. The remaining pyrrole was removed by vacuum distillation with gentle heating. The product was purified by silica gel column chromatography (CH_2Cl_2/hexane/Et_3N 50:49:1) to afford **DPM-1c** quantitatively as a red solid. R_f=0.85 (CH_2Cl_2); ^{1}H NMR (600 MHz, $CDCl_3$, 20°C): δ=7.91 (brs, 4H; NH), 7.66–7.65 (m, 4H; ArH), 7.50 (m, 1H; ArH), 7.45–7.41 (m, 6H; ArH), 7.29 (t, J=8.4 Hz, 2H; ArH), 7.20 (m, 1H; ArH), 5.81 (dd, J=2.4 Hz, 4H; pyrrole-H), 5.75 (dd, J=2.4, 2.4 Hz, 4H; pyrrole-H), 5.36 (s, 2H; *meso*-H), 2.52 (t, J=7.8 Hz, 8H; $CH_2C_{14}H_{28}CH_3$), 1.24 (m, 112H; $CH_2C_{14}H_{28}CH_3$), 0.87 ppm (m, 12H; $CH_2C_{14}H_{28}CH_3$); ESI-TOF-MS (observed with the existence of both $AgClO_4$ and TCNQ as matrix): m/z (%): calcd for $C_{104}H_{158}N_4$+Ag: 1570.15; found: 1570.2 $[M+Ag]^+$ (68), 1571.1 $[M+Ag+1]^+$ (59), 1572.1 $[M+Ag+2]^+$ (100), 1573.2 $[M+Ag+3]^+$ (75), 1574.2 $[M+Ag+4]^+$ (54).

1,3-Bis(5,5′-(dimethyl)dipyrrilylphenylethynyl)benzene (1b): Dipyrromethane **DPM-1b** (67.2 mg, 0.108 mmol) dissolved in THF (20 mL) was stirred, and DDQ (48.9 mg, 0.215 mmol) was slowly added. The reaction mixture was purified by alumina and silica gel column chromatography (CH_2Cl_2) to afford **1b** (48.2 mg, 72%) as a dark red solid. R_f=0.40 (5% MeOH/CH_2Cl_2); ^{1}H NMR (600 MHz, $CDCl_3$, 20°C): δ=7.71 (m, 1H; ArH), 7.63 (m, 2H; ArH), 7.60 (ddd, J=7.2, 1.2, 1.2 Hz, 2H; ArH), 7.43–7.42 (m, 4H; ArH), 7.40 (dd, J=7.8, 7.8 Hz, 1H; ArH), 6.45 (d, J=4.2 Hz, 4H; pyrrole-H), 6.17 (d, J=4.2 Hz, 4H; pyrrole-H), 2.45 ppm (s, 12H; CH_3); UV/Vis ($CHCl_3$): λ_{max} ($\varepsilon\times10^{-5}$)=446 nm (0.39 M^{-1} cm^{-1}); FABMS: m/z (%): calcd for $C_{44}H_{34}N_4$: 618.28; found: 619.4 $[M+1]^+$ (100), 620.4 $[M+2]^+$ (64).

1,3-Bis(5,5′-bis(hexadecyl)dipyrrilylphenylethynyl)benzene (1c): Dipyrromethane **DPM-1c** (44.4 mg, 0.03 mmol) was dissolved in THF (15 mL). DDQ (13.8 mg, 0.06 mmol) was added and stirred 10 min. The reaction mixture was purified by alumina and silica gel column chromatography (CH_2Cl_2) to afford **1c** (31.2 mg, 70%) as a dark red solid. R_f=0.53 (CH_2Cl_2); ^{1}H NMR (600 MHz, $CDCl_3$, 20°C): δ=7.70 (dd, J=1.8, 1.2 Hz, 1H; ArH), 7.64 (s, 1H; ArH), 7.59 (ddd, J=7.8, 1.2, 1.2 Hz, 2H; ArH), 7.48 (dd, J=8.4, 1.8 Hz, 2H; ArH), 7.45–7.43 (m, 2H; ArH), 7.40 (t, J=7.8 Hz, 2H; ArH), 7.33 (t, J=8.4 Hz, 1H; ArH), 6.47 (d, J=4.2 Hz, 4H; pyrrole-H), 6.18 (d, J=4.2 Hz, 4H; pyrrole-H), 2.74 (t, J=7.8 Hz, 8H; $CH_2C_{14}H_{28}CH_3$), 1.25 (m, 112H; $CH_2C_{14}H_{28}CH_3$), 0.87 ppm (t, J=7.2 Hz, 12H; $CH_2C_{14}H_{28}CH_3$); UV/Vis ($CHCl_3$): λ_{max} ($\varepsilon\times10^{-5}$)=450 nm (0.41 M^{-1} cm^{-1}); FABMS: m/z (%): calcd for $C_{104}H_{154}N_4$: 1459.22; found: 1460.8 $[M+1]^+$ (100), 1461.7 $[M+2]^+$ (79).

Zn^{II} complex of 1a (1a$_2$·Zn$_2$): $Zn(OAc)_2$·$2H_2O$ (11.4 mg, 0.05 mmol) was added to a $CHCl_3$ solution (25 mL) of dipyrrin **1a** (28.0 mg, 0.05 mmol) and pyrene (5.2 mg, 0.03 mmol), and the reaction mixture was heated at reflux temperature for 47 h. The solution was evaporated and purified by silica gel column chromatography (5% MeOH/$CHCl_3$) and recrystallized from $CHCl_3$/hexane to afford **1a**$_2$·Zn_2 (24.1 mg, 77%) as a yellow solid. R_f=0.62 (3% MeOH/CH_2Cl_2); ^{1}H NMR (600 MHz, $CDCl_3$, 20°C): δ=7.77–7.72 (m, 6H; ArH), 7.67–7.64 (m, 4H; ArH), 7.58–7.50 (m, 16H; ArH, pyrrole-H), 7.47–7.45 (m, 4H; ArH), 7.39–7.36 (m, 2H; ArH), 6.79–6.70 (m, 8H; pyrrole-H), 6.43–6.41 ppm (m, 8H; pyrrole-H); UV/Vis ($CHCl_3$): λ_{max} ($\varepsilon\times10^{-5}$)=486 nm (2.2 M^{-1} cm^{-1}); ESI-TOF-MS: m/z (%): calcd for $C_{80}H_{48}N_8Zn_2$+H: 1249.27; found: 1249.3 $[M+H]^+$ (59), 1250.3 $[M+H+1]^+$ (57), 1251.3 $[M+H+2]^+$ (90), 1252.3 $[M+H+3]^+$ (83), 1253.3 $[M+H+4]^+$ (100), 1254.3 $[M+H+5]^+$ (76), 1255.3 $[M+H+6]^+$ (56), 1256.3 $[M+H+7]^+$ (33), 1257.3 $[M+H+8]^+$ (25), 1258.3 $[M+H+9]^+$ (19); calcd for $C_{80}H_{48}N_8Zn_2$+Ag: 1355.16; found: 1355.2 $[M+Ag]^+$ (34), 1356.2 $[M+Ag+1]^+$ (31), 1357.2 $[M+Ag+2]^+$ (80), 1358.2 $[M+Ag+3]^+$ (66), 1359.2 $[M+Ag+4]^+$ (100), $[M+Ag+5]^+$ 1360.2 (78), 1361.2 $[M+Ag+6]^+$ (81), 1362.2 $[M+Ag+7]^+$ (57), 1363.2 $[M+Ag+8]^+$ (40), 1364.2 $[M+Ag+9]^+$ (25), 1365.2 $[M+Ag+10]^+$ (15).

Cu^{II} complex of 1a (1a$_2$·Cu$_2$): $Cu(OAc)_2$ (24.3 mg, 0.13 mmol) was added to a $CHCl_3$ solution (60 mL) of dipyrrin **1a** (74.8 mg, 0.13 mmol) and pyrene (13.7 mg, 0.07 mmol), and the reaction mixture was heated at reflux temperature for 2 h. The solution was evaporated and purified by silica gel column chromatography (10% hexane/$CHCl_3$) and recrystallized from $CHCl_3$/hexane to afford **1a**$_2$·Cu_2 (59.1 mg, 71%) as a dark red solid. R_f=0.84 (1% MeOH/CH_2Cl_2); UV/Vis ($CHCl_3$): λ_{max} ($\varepsilon\times10^{-5}$)=469 nm (1.5 M^{-1} cm^{-1}); ESI-TOF-MS: m/z (%): calcd for $C_{80}H_{48}Cu_2N_8$+H: 1247.27; found: 1247.3 $[M+H]^+$ (89), 1248.3 $[M+H+1]^+$ (90), 1249.3 $[M+H+2]^+$ (100), 1250.3 $[M+H+3]^+$ (73), 1251.3 $[M+H+4]^+$ (35), 1252.3 $[M+H+5]^+$ (25), 1253.3 $[M+H+6]^+$ (14); calcd for $C_{80}H_{48}Cu_2N_8$+Ag: 1353.16; found: 1353.2 $[M+Ag]^+$ (43), 1354.2 1353.2 $[M+Ag+1]^+$ (38), 1355.2 $[M+Ag+2]^+$ (100), 1356.2 $[M+Ag+3]^+$ (78), 1357.2 $[M+Ag+4]^+$ (75), 1358.2 $[M+Ag+5]^+$ (51), 1359.2 $[M+Ag+6]^+$ (31), 1360.2 $[M+Ag+7]^+$ (14).

Ni^{II} complex of 1a (1a$_2$·Ni$_2$): $Ni(OAc)_2$·$4H_2O$ (34.4 mg, 0.14 mmol) was added to a $CHCl_3$ solution (60 mL) of dipyrrin **1a** (77.7 mg, 0.14 mmol) and pyrene (14.0 mg, 0.07 mmol), and the reaction mixture was heated at reflux temperature for 24 h. The solution was evaporated and purified by silica gel column chromatography (3% MeOH/$CHCl_3$) and recrystallized from $CHCl_3$/hexane to afford **1a**$_2$·Ni_2 (74.5 mg, 87%) as a dark red solid. R_f=0.38 (1% MeOH/CH_2Cl_2); ^{1}H NMR (600 MHz, $CDCl_3$, 20°C): δ=9.29 (brs, 8H; pyrrole-H), 7.74 (s, 2H; ArH), 7.61–7.60 (m, 8H; ArH), 7.48 (d, J=8.4 Hz, 4H; ArH), 7.43–7.34 (m, 18H; ArH+pyrrole-H), 6.77 ppm (brs, 8H; pyrrole-H); UV/Vis ($CHCl_3$): λ_{max} ($\varepsilon\times10^{-5}$)=476 nm (0.89 M^{-1} cm^{-1}); ESI-TOF-MS: m/z (%): calcd for $C_{80}H_{48}N_8Ni_2$+Ag: 1343.18; found: 1343.2 $[M+Ag]^+$ (52), 1344.2 $[M+Ag+1]^+$ (57), 1345.2 $[M+Ag+2]^+$ (100), 1346.2 $[M+Ag+3]^+$ (89), 1347.2 $[M+Ag+4]^+$ (83), 1348.1 $[M+Ag+5]^+$ (70), 1349.2 $[M+Ag+6]^+$ (43), 1350.2 $[M+Ag+7]^+$ (35), 1351.1 $[M+Ag+8]^+$ (27).

Zn^{II} complex of 1b (1b$_2$·Zn$_2$): $Zn(OAc)_2$·$2H_2O$ (8.2 mg, 0.037 mmol) was added to a $CHCl_3$ solution (20 mL) of dipyrrin **1b** (23.1 mg, 0.037 mmol) and pyrene (3.8 mg, 0.019 mmol), and the reaction mixture was heated at reflux temperature for 4 h. The solution was evaporated and purified by silica gel column chromatography (5% MeOH/$CHCl_3$) and recrystallized from $CHCl_3$/hexane to afford **1b**$_2$·Zn_2 (12.6 mg, 49%) as a dark red solid. R_f=0.93 (5% hexane/CH_2Cl_2); ^{1}H NMR (600 MHz, $CDCl_3$, 20°C): δ=7.74–7.60 (m, 10H; ArH), 7.53–7.49 (m, 8H; ArH), 7.43–7.40 (m, 4H; ArH), 7.38–7.35 (m, 2H; ArH), 6.64–6.55 (m, 8H; pyrrole-H), 6.23–6.19 (m, 8H; pyrrole-H), 2.16–2.05 ppm (m, 24H; CH_3); UV/Vis ($CHCl_3$): λ_{max} ($\varepsilon\times10^{-5}$)=493.0 nm (2.3 M^{-1} cm^{-1}); FABMS: m/z (%): 1363.3 $[M+3]^+$ (77), 1364.3 $[M+4]^+$ (100), 1365.2 $[M+5]^+$ (77); ESI-TOF-MS: m/z (%): calcd for $C_{88}H_{64}N_8Zn_2$+H: 1361.39; found: 1361.4 $[M+H]^+$ (92), 1362.4 $[M+H+1]^+$ (85), 1363.4 $[M+H+2]^+$ (87), 1364.4 $[M+H+3]^+$ (100), 1365.4 $[M+H+4]^+$ (97), 1366.4 $[M+H+5]^+$ (77), 1367.4 $[M+H+6]^+$ (58), 1368.4 $[M+H+7]^+$ (34), 1369.4 $[M+H+8]^+$ (29), 1370.4 $[M+H+9]^+$ (18); calcd for $C_{88}H_{64}N_8Zn_2$+Ag: 1467.29; found: 1467.3 $[M+Ag]^+$ (31), 1468.3 $[M+Ag+1]^+$ (31), 1469.3 $[M+Ag+2]^+$ (73), 1470.3 $[M+Ag+3]^+$ (73), 1471.3 $[M+Ag+4]^+$ (100), 1472.3 $[M+Ag+5]^+$ (82), 1473.3 $[M+Ag+6]^+$ (90), 1474.3 $[M+Ag+7]^+$ (58), 1475.3 $[M+Ag+8]^+$ (47), 1476.3 $[M+Ag+9]^+$ (29), 1477.3 $[M+Ag+10]^+$ (18),

Zn^{II} complex of 1c (1c$_2$·Zn$_2$): $Zn(OAc)_2$·$2H_2O$ (4.7 mg, 0.02 mmol) was added to a $CHCl_3$ solution (25 mL) of dipyrrin **1c** (31.2 mg, 0.02 mmol) and pyrene (2.4 mg, 0.01 mmol), and the reaction mixture was heated at reflux temperature for 10 h. The solution was evaporated and purified by silica gel column chromatography (50% hexane/CH_2Cl_2) to afford **1c**$_2$·Zn_2 (13.1 mg, 40%) as a dark red oil. R_f=0.89 (CH_2Cl_2); ^{1}H NMR (600 MHz, $CDCl_3$, 20°C): δ=7.74–7.71 (m, 2H; ArH), 7.68–7.67 (m, 4H; ArH), 7.62–7.59 (m, 4H; ArH), 7.50–7.46 (m, 8H; ArH), 7.41–7.38 (m, 4H; ArH), 7.36–7.34 (m, 2H; ArH), 6.62–6.55 (m, 8H; pyrrole-H), 6.23–

6.19 (m, 8H; pyrrole-H), 2.41–2.36 (m, 16H; $CH_2C_{14}H_{28}CH_3$), 1.25–1.08 (m, 224H; $CH_2C_{14}H_{28}CH_3$), 0.89–0.85 ppm (m, 24H; $CH_2C_{14}H_{28}CH_3$); UV/Vis ($CHCl_3$): λ_{max} ($\varepsilon \times 10^{-5}$) = 496.0 nm ($1.9\,M^{-1}\,cm^{-1}$); MALDI-TOF-MS: *m*/*z* (%): calcd for $C_{208}H_{304}N_8Zn_2$: 3042.26; found: 3045.8 $[M+3]^+$ (91), 3048.6 $[M+6]^+$ (100).

Optimized structure: AM1 calculations of **1a**,**b**$_2$·Zn_2 ($\Lambda\Delta$-type) and **1a**,**b**$_2$·Zn_2 ($\Lambda\Lambda$-type) were carried out using Gaussian 03 program[15] and an HP Compaq dc5100 SFF computer.

X-ray crystallography: Data was collected on a Bruker SMART CCDC for **1a**$_2$·Zn_2, refined by full-matrix least-squares procedures with anisotropic thermal parameters for the non-hydrogen atoms. The hydrogen atoms were calculated in ideal positions. Solutions of the structures were performed by using the Crystal Structure crystallographic software package (Molecular Structure Corporation).

Crystal data for **1a**$_2$·Zn_2 (from THF/chlorobenzene/hexane): $C_{88}H_{64}N_8O_2Zn_2$, M_w = 1396.21, monoclinic, *C*2/*c* (no.15), a = 36.946(13), b = 17.364(5), c = 11.406(4) Å, β = 106.119(13)°, V = 7029(4) Å^3, T = 123(2) K, Z = 4, ρ_{calcd} = 1.319 g cm^{-3}, $\mu(Mo_{K\alpha})$ = 0.739 mm^{-1}, reflections collected = 54701, independent reflections = 14022 (R_{int} = 0.1120), R_1 = 0.0884, wR_2 = 0.1816, GOF = 0.987 ($I > 2\sigma(I)$). CCDC-635600 contains the supplementary crystallographic data for this paper. These data can be obtained free of charge from The Cambridge Crystallographic Data Centre via www.ccdc.cam.ac.uk/data_request/cif.

Acknowledgements

This work was supported by the "Academic Frontier" Project for Private Universities, namely, the matching fund subsidy from MEXT, 2003–2008, Saneyoshi Scholarship Foundation, and the Japan Securities Scholarship Foundation. We thank Professor Atsuhiro Osuka, Mr. Shigeki Mori and Mr. Shohei Saito, Kyoto University, for X-ray analysis, Professor Hiroshi Shinokubo, Mr. Satoru Hiroto, and Mr. Chihiro Maeda, Kyoto University, for ESI-TOF-MS and HPLC analyses, Dr. Tomohiro Miyatake, Ryukoku University, for FAB-MS measurements, and Professor Hitoshi Tamiaki, Professor Tadashi Mizoguchi, and Dr. Michio Kunieda, Ritsumeikan University, for helpful discussions.

[1] a) *Transition Metals in Supramolecular Chemistry*, (Ed.: J.-P. Sauvage), Wiley, Chichester, **1999**; b) S. Leininger, B. Olenyuk, P. J. Stang, *Chem. Rev.* **2000**, *100*, 853–908; c) P. J. Stang, B. Olenyuk, *Acc. Chem. Res.* **1997**, *30*, 502–518; d) M. Fujita, K. Umemoto, M. Yoshizawa, N. Fujita, T. Kusukawa, K. Biradha, *Chem. Commun.* **2001**, 509–518; e) S. Kitagawa, R. Kitaura, S. Noro, *Angew. Chem.* **2004**, *116*, 2388–2430; *Angew. Chem. Int. Ed.* **2004**, *43*, 2334–2375.

[2] a) R. Kitaura, S. Kitagawa, Y. Kubota, T. C. Kobayashi, K. Kindo, Y. Mita, A. Matsuo, M. Kobayashi, H.-C. Chang, T. C. Ozawa, M. Suzuki, M. Sakata, M. Takata, *Science* **2002**, *298*, 2358–2361; b) R. Matsuda, R. Kitaura, S. Kitagawa, Y. Kubota, R. V. Belosludov, T. C. Kobayashi, H. Sakamoto, T. Chiba, M. Takata, Y. Kawazoe, Y. Mita, *Nature* **2005**, *436*, 238–241.

[3] a) M. Eddaoudi, J. Kim, N. Rosi, D. Vodak, J. Wachter, M. O'Keeffe, O. M. Yaghi, *Science* **2002**, *295*, 469–472; b) J. L. C. Rowsell, J. Eckert, O. M. Yaghi, *J. Am. Chem. Soc.* **2005**, *127*, 14904–14910; c) A. R. Millward, O. M. Yaghi, *J. Am. Chem. Soc.* **2005**, *127*, 17998–17999.

[4] a) T. Yamamoto, A. M. Arif, P. J. Stang, *J. Am. Chem. Soc.* **2003**, *125*, 12309–12317; b) H. B. Yang, N. Das, F. Huang, A. M. Hawkridge, D. C. Muddiman, P. J. Stang, *J. Am. Chem. Soc.* **2006**, *128*, 10014–10015.

[5] a) M. Fujita, D. Oguro, M. Miyazawa, H. Oka, K. Yamaguchi, K. Ogura, *Nature* **1995**, *378*, 469–471; b) S. Sato, J. Iida, K. Suzuki, M. Kawano, T. Ozeki, M. Fujita, *Science* **2006**, *313*, 1273–1276.

[6] a) H. Jiang, W. Lin, *J. Am. Chem. Soc.* **2003**, *125*, 8084–8085; b) H. Jiang, W. Lin, *J. Am. Chem. Soc.* **2004**, *126*, 7426–7427.

[7] a) H. Fischer, H. Orth, *Die Chemie des Pyrrols, Vol. 2*, Akademische Verlagsgesellschaft, Leipzig (Germany), **1937**; b) H. Falk, *The Chemistry of Linear Oligopyrroles and Bile Pigments*, Springer, Vienna (Austria), **1989**.

[8] a) Y. Zhang, A. Thompson, S. J. Rettig, D. Dolphin, *J. Am. Chem. Soc.* **1998**, *120*, 13537–13538; b) A. Thompson, S. J. Rettig, D. Dolphin, *Chem. Commun.* **1999**, 631–632; c) A. Thompson, D. Dolphin, *Org. Lett.* **2000**, *2*, 1315–1318; d) A. Thompson, D. Dolphin, *J. Org. Chem.* **2000**, *65*, 7870–7877; e) Q, Chen, Y. Zhang, D. Dolphin, *Tetrahedron Lett.* **2002**, *43*, 8413–8416.

[9] a) S. R. Halper, S. M. Cohen, *Chem. Eur. J.* **2003**, *9*, 4661–4669; b) S. R. Halper, M. R. Malachowski, H. M. Delaney, S. M. Cohen, *Inorg. Chem.* **2004**, *43*, 1242–1249; c) S. R. Halper, S. M. Cohen, *Angew. Chem.* **2004**, *116*, 2439–2442; *Angew. Chem. Int. Ed.* **2004**, *43*, 2385–2388; d) L. Do, S. R. Halper, S. M. Cohen, *Chem. Commun.* **2004**, 2662–2663; e) S. R. Halper, L. Do, J. R. Stork, S. M. Cohen, *J. Am. Chem. Soc.* **2006**, *128*, 15255–15268.

[10] L. Yu, K. Muthukumaran, I. V. Sazanovich, C. Kirmaier, E. Hindin, J. R. Diers, P. D. Boyle, D. F. Bocian, D. Holten, J. S. Lindsey, *Inorg. Chem.* **2003**, *42*, 6629–6647.

[11] H. Maeda, M. Ito, *Chem. Lett.* **2005**, *34*, 1150–1151.

[12] H. Maeda, M. Hasegawa, T. Hashimoto, T. Kakimoto, S. Nishio, T. Nakanishi, *J. Am. Chem. Soc.* **2006**, *128*, 10024–10025.

[13] a) L. Yang, Y. Zhang, G. Yang, Q. Chen, J. S. Ma, *Dyes Pigm.* **2004**, *62*, 27–33; b) T. E. Wood, N. D. Dalgleish, E. D. Power, A. Thompson, X. Chen, Y. Okamoto, *J. Am. Chem. Soc.* **2005**, *127*, 5740–5741.

[14] a) G. Seeber, B. E. F. Tiedemann, K. N. Raymond, *Top. Curr. Chem.* **2006**, *265*, 147–183; b) Although dipyrrin–Zn^{II} complex in which two dipyrrin moieties are almost perpendicular is known to exhibit no chirality, we define configurations Λ and Δ by the moieties including dipyrrin and the neighboring *meso*-aryl moiety, which is tilted at ca. 45° to the dipyrrin plane, as shown below.

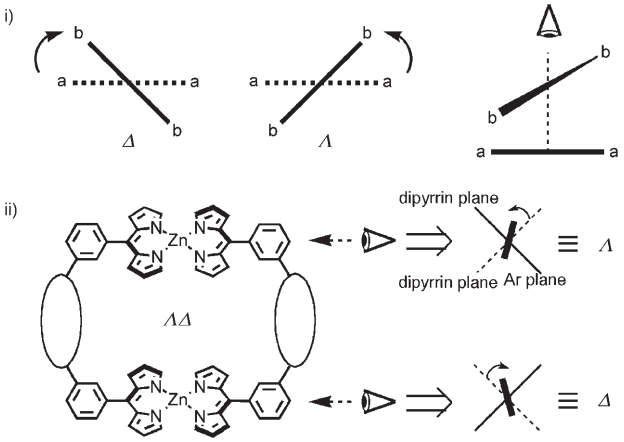

[15] Gaussian 03, Revision C.01, M. J. Frisch, G. W. Trucks, H. B. Schlegel, G. E. Scuseria, M. A. Robb, J. R. Cheeseman, J. A. Montgomery, Jr., T. Vreven, K. N. Kudin, J. C. Burant, J. M. Millam, S. S. Iyengar, J. Tomasi, V. Barone, B. Mennucci, M. Cossi, G. Scalmani, N. Rega, G. A. Petersson, H. Nakatsuji, M. Hada, M. Ehara, K. Toyota, R. Fukuda, J. Hasegawa, M. Ishida, T. Nakajima, Y. Honda, O. Kitao, H. Nakai, M. Klene, X. Li, J. E. Knox, H. P. Hratchian, J. B. Cross, C. Adamo, J. Jaramillo, R. Gomperts, R. E. Stratmann, O. Yazyev, A. J. Austin, R. Cammi, C. Pomelli, J. W. Ochterski, P. Y. Ayala, K. Morokuma, G. A. Voth, P. Salvador, J. J. Dannenberg, V. G. Zakrzewski, S. Dapprich, A. D. Daniels, M. C. Strain, O. Farkas, D. K. Malick, A. D. Rabuck, K. Raghavachari, J. B. Foresman, J. V. Ortiz, Q. Cui, A. G. Baboul, S. Clifford, J. Cioslowski, B. B. Stefanov, G. Liu, A. Liashenko, P. Piskorz, I. Komaromi, R. L. Martin, D. J. Fox, T. Keith, M. A. Al-Laham, C. Y. Peng, A. Na-

nayakkara, M. Challacombe, P. M. W. Gill, B. Johnson, W. Chen, M. W. Wong, C. Gonzalez, J. A. Pople, Gaussian, Inc., Wallingford CT, **2004**.

[16] Under this HPLC condition, one of the minor "two" peaks derived from the chiral stereoisomers of $\mathbf{1a}_2{\cdot}Zn_2$ overlaps with the major single peak of the achiral isomer, as suggested from the UV/Vis absorption spectra (which differ in two stereoisomers), during the analysis. See Supporting Information.

[17] The equilibrium constants K between the chiral and *meso* isomers of $C_{16}H_{33}$-substituted $\mathbf{1c}_2{\cdot}Zn_2$ at 60, 20, and $-20\,^{\circ}C$ are 5.4, 4.6, and 4.4, respectively, with the corresponding ΔG^0 of -4.1, -3.7, and $-3.6\,kJ\,mol^{-1}$. By using van 't Hoff plots, the thermodynamic parameters (ΔH^0 and ΔS^0) of $\mathbf{1c}_2{\cdot}Zn_2$ are estimated to be $1.7\,kJ\,mol^{-1}$ and $19\,J\,K^{-1}\,mol^{-1}$, which are similar to those of $\mathbf{1a}_2{\cdot}Zn_2$ and $\mathbf{1b}_2{\cdot}Zn_2$. The derivative with long alkyl substituents at the dipyrrin units also seems to enable the interconversion between the two stereoisomers, possibly due to the flexible aliphatic chains.

[18] Under the irradiation of one of the internal β-CH protons of the minor isomer for 60 s and using the hypothetical equation $\frac{d(M_{Ai}+M_{Ae})}{dt}=-k_A(M_{Ai}+M_{Ae})+k_B(M_{Bi}+M_{Be})+\frac{M_{0Ai}-M_{Ai}}{T_{1Ai}}+\frac{M_{0Ae}-M_{Ae}}{T_{1Ae}}$ (M_{Ai}: the magnetization of the internal β-CH protons of the major isomer (A); M_{Ae}: the magnetization of the external β-CH protons of the major isomer; M_{Bi}: the magnetization of the internal β-CH protons of the minor isomer (B); M_{Be}: the magnetization of the external β-CH protons of the minor isomer; M_{0Ai}: the magnetization of the internal β-CH protons of the major isomer at thermal equilibrium state; M_{0Ae}: the magnetization of the external β-CH protons of the major isomer at thermal equilibrium state; T_{1Ai}: the relaxation time of the internal β-CH protons of the major isomer; T_{1Ae}: the relaxation time of the external β-CH protons of the major isomer; k_A: the rate constant from the major to minor isomer; k_B: the rate constant from the minor to major isomer) and the conditions such as $\frac{d(M_{Ai}+M_{Ae})}{dt}$, $M_{Bi}=0$, $T_{1Ai}=T_{1Ae}=T_{1A}$ (by measurements), and $k_B=K{\cdot}k_A$ (K: equilibrium constant between the major and minor isomers), the rate constant k_A can be estimated as shown below: $k_A=\frac{(M_{0Ai}-M_{Ai})+(M_{0Ae}-M_{Ae})}{T_{1A}\times\{(M_{Ai}+M_{Ae})-K{\cdot}M_{Be}\}}$. It affords the values of 0.5 ($\mathbf{1a}_2{\cdot}Zn_2$) and $0.3\,s^{-1}$ ($\mathbf{1b}_2{\cdot}Zn_2$), respectively.

[19] a) M. Oki, *The Chemistry of Rotational Isomers*, Springer, Berlin (Germany), **1993**; b) T. R. Kelly, M. C. Bowyer, K. V. Bhaskar, D. Bebbington, A. Garcia, F. Lang, M. H. Kim, M. P. Jette, *J. Am. Chem. Soc.* **1994**, *116*, 3657–3658; c) T. Bedart, J. S. Moore, *J. Am. Chem. Soc.* **1995**, *117*, 10662–10671; d) V. Balzani, A. Credi, F. M. Raymo, J. F. Stoddart, *Angew. Chem.* **2000**, *112*, 3484–3530; *Angew. Chem. Int. Ed.* **2000**, *39*, 3348–3391; e) V. Balzani, M. Venturi, A. Credi, *Molecular Devices and Machines; A Journey to the Nanoworld*, Wiley-VCH, Weinheim (Germany), **2003**.

[20] J. Rebek, Jr., *Angew. Chem.* **2005**, *117*, 2104–2115; *Angew. Chem. Int. Ed.* **2005**, *44*, 2068–2078.

Received: March 22, 2007
Published online: July 3, 2007

